COMPARISON OF EXPERIMENTAL
AND CALCULATED CRITICAL MASSES
FOR A GAS CORE CAVITY REACTOR

by Klaus H. Gumto

Lewis Research Center
Cleveland, Ohio 44135

1. Report No. NASA TM X-2055	2. Government Accession No.	3. Recipient's Catalog No.
4. Title and Subtitle COMPARISON OF EXPERIMENTAL AND CALCULATED CRITICAL MASSES FOR A GAS CORE CAVITY REACTOR		5. Report Date July 1970
		6. Performing Organization Code
7. Author(s) Klaus H. Gumto		8. Performing Organization Report No. E-5320
9. Performing Organization Name and Address Lewis Research Center National Aeronautics and Space Administration Cleveland, Ohio 44135		10. Work Unit No. 122-29
		11. Contract or Grant No.
		13. Type of Report and Period Covered
12. Sponsoring Agency Name and Address National Aeronautics and Space Administration Washington, D.C. 20546		Technical Memorandum
		14. Sponsoring Agency Code

16. Abstract

Experimental critical masses for a cylindrical cavity reactor with simulated gaseous fuel are compared with calculated critical masses for similar reactor configurations. Both diffusion and one- and two-dimensional transport theory computer codes were employed in five distinct sets of calculations. By varying input parameters such as number of broad energy groups and number of mesh intervals from one set to another, the effect of the changes on the accuracy of the calculations was determined.

17. Key Words (Suggested by Author(s)) Cavity reactor Gas core Nuclear analysis	18. Distribution Statement Unclassified - unlimited		
19. Security Classif. (of this report) Unclassified	20. Security Classif. (of this page) Unclassified	21. No. of Pages 22	22. Price* $3.00

COMPARISON OF EXPERIMENTAL AND CALCULATED CRITICAL

MASSES FOR A GAS CORE CAVITY REACTOR

by Klaus H. Gumto

Lewis Research Center

SUMMARY

This report presents the results of a comparison of calculated and experimental critical masses for a gas core cavity reactor. The comparison points out sources of error in the calculations and provides guidelines for further calculations.

This study uses the results of a series of experiments, conducted at the National Reactor Test Station, for comparison with analytical results. The calculations were performed on an IBM 7094 computer using both diffusion theory and transport theory codes. The transport theory calculations were made in cylindrical and spherical geometry, while the diffusion calculations were restricted to spherical geometry only. Input parameters included energy groups, P_0 and P_1 scatter-transfer cross sections, up and down scattering, number of materials and mesh interval spacing. The analysis covered the range of fuel radius to cavity radius ratios from 0.500 to 0.900.

The results indicate that the transport theory approximations used in this study overestimated the critical masses, while the diffusion calculations underestimated them. The deviation of the critical masses calculated with one-dimensional diffusion theory codes from the experimental critical masses was inversely proportional to the radius ratio. This points out the relative inability of diffusion theory to handle large voids. It also indicates that as the fuel radius is reduced, that is, as the radius ratio decreases, it becomes more difficult to approximate the fuel cylinder by a sphere. This problem also arose in the one-dimensional transport calculations, but it did not produce as large a deviation between the calculated and experimental critical masses as resulted from the diffusion calculations. Therefore, the one-dimensional transport calculations were more accurate at smaller radius ratio than the diffusion calculations.

The two-dimensional (cylindrical geometry) transport calculations had excessively long computer running times (several hours) and large critical mass deviations. These derivations were mainly due to lack of spatial and energy group definition imposed by computer storage limits. This problem did not arise in the one-dimensional calculations. Two-dimensional calculations will require optimization of input parameters and adequate core storage in order to get accurate results, although there is little prospect of significant reduction in computer time.

INTRODUCTION

The gas-core cavity reactor is potentially one of the most efficient means of space propulsion. The promise of high specific impulse has prompted numerous analytical studies of such power sources. On the other hand, experimental data on gas-core cavity reactors are scarce. To date, only two cavity reactors have been constructed and operated in the United States: one at Los Alamos and the other at the National Reactor Test Station (LPT). Both reactors simulated a true gaseous core by various means, and neither reactor was operated at the high temperatures which are expected in an operating gas core rocket reactor. Since previous analytical studies were based on mathematical approximations to theory, it was not certain that the results of these calculations were representative of an actual reactor.

In order to determine whether the critical mass of a gas-core cavity reactor could be calculated accurately, a series of calculations was performed at Lewis. Three configurations of the reactor at the National Reactor Test Station were used for the comparison. The calculations used the same geometry and materials as the experiment, with the exception that a homogeneous medium simulating gaseous uranium was assumed in the calculations instead of the UO_2 foils used to simulate gaseous fuel in the experiment.

The calculations were made in five distinct sets. Set 1, the initial calculations, used diffusion theory. In order to improve the results, transport theory was substituted. Sets 2 and 3 used a two-dimensional cylindrical geometry, while sets 4 and 5 had a one-dimensional, or spherical, geometry. These set numbers will be used throughout the report to identify each series of calculations.

Within the transport calculations, several parameters were changed from one set to another in order to approximate the experimental results more closely. These included the change in geometry, mesh spacing, number and spacing of energy groups and number of distinct regions. In addition, the effects of up and down scattering transfers and P_0 against P_1 cross sections were investigated. The comparison of the resulting critical masses with those obtained from the experiments provided a measure of the accuracy of the calculations and the effect of the changes. Henderson and Kunze (ref. 1) applied some of the conclusions of this study in their more detailed analysis of both the configurations in this report and those of later critical experiments with gaseous UF_6 fuel.

An IBM 7044/7094-II direct couple computer was used to perform all calculations. All computer runs were made with existing codes and cross section libraries.

SYMBOLS

D   diameter

k   multiplication factor

k_{eff} effective multiplication factor

L   length

m   fuel mass

P   Legendre polynomial expansion term

CALCULATIONAL PROCEDURES

Reactor Configuration

The reactor consisted of a cylindrical cavity 122 centimeters long and 183 centimeters in diameter, resulting in a cavity volume of 3.2×10^6 cubic centimeters and a length-to-diameter ratio of 2/3. The cavity was formed by the inner walls of annular aluminum tank which surrounded the cavity with an 89-centimeter layer of D_2O as reflector and moderator. Aluminum structure weighing 764 kilograms was inside the tank. The tank was made in two parts, with one end on a movable table. This provided access to the cavity, but also introduced an air gap at the separation plane. The movable end reflector also contained a hole 30 centimeters in diameter to simulate an exhaust nozzle. However, this hole was closed with a D_2O filled plug for the configurations in this report. An aluminum support structure filled the cavity. This permitted the arrangement of the UO_2 fuel sheets in a three-dimensional lattice which simulated gaseous fuel. These UO_2 foils were 0.00254 centimeter thick, and were 93.2 percent enriched with U^{235} (ref. 2).

Three of the experimental fuel arrangements were selected for comparison. All consisted of foils so located that they formed a cylinder as long as, and concentric with, the cavity. Only the cylinder radius varied. The fuel radius to cavity radius ratios were 0.890, 0.667, and 0.530.

Analytical Model

The analytical model is simplified from the experimental reactor in order to reduce the complexity of the calculations (fig. 1). This results in complete homogeneity
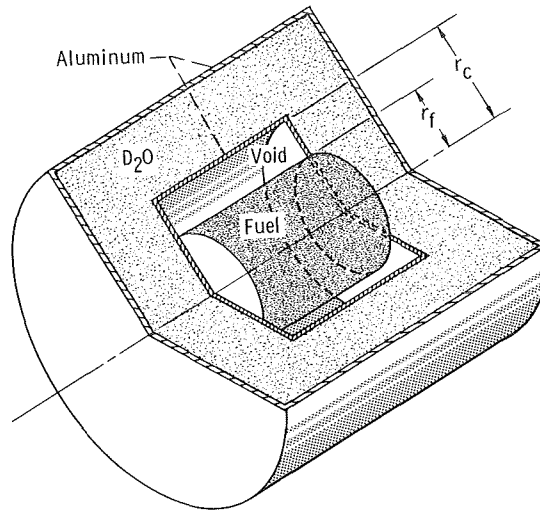
Figure 1. - Model of cavity reactor.

in each of the regions of the model reactor as compared to the discrete materials in the actual reactor. Also, the plugged exhaust nozzle and the air gap were eliminated from the model. The aluminum fuel support structure was homogenized over the entire cavity volume. For the model, this consisted of 34-kilogram aluminum with 0.51 kilogram of manganese impurity. The constituents of the UO_2 foils were homogenized over the fuel region which also contained part of the aluminum support structure. All materials were considered to be at room temperature for the calculations.

Since the experimental reactor was under construction at the time the analysis was started, the dimensions used were those currently available. Thus they will vary slightly from one set of calculations to another and from the published final dimensions of the experimental reactor. These variations are small, however, and do not significantly affect any calculations. Tables I to III give the dimensions used in each set of calculations.

In general, five regions were used

(1) The fuel region, containing both fuel and support structure, with the fueled radius ranging from 0.5 to 0.89 of the cavity radius.

(2) The void region, which is the annular space between the fuel and the cavity wall, containing only aluminum support structure.

(3) The inner wall of the D_2O tank, which also forms the cavity and is made of aluminum.

(4) The D_2O with 0.25 percent H_2O impurity and 693 kilograms of aluminum, all homogenized over the entire region.

(5) The outer tank wall, also made of aluminum.

4

TABLE I. - MATERIALS AND GEOMETRY FOR

ONE-DIMENSIONAL DIFFUSION

CALCULATIONS - SET 1

Distance to outer edge of region, cm	Number of mesh points	Width of mesh cell, cm	Material
Fuel radius to cavity radius ratio, 0.890			
81.30	35	2.323	Fuel
91.34	5	2.007	Void
92.86	3	.507	Aluminum
184.30	40	2.268	D_2O
185.82	3	.507	Aluminum
Fuel radius to cavity radius ratio, 0.667			
60.97	35	1.742	Fuel
91.45	5	6.097	Void
92.97	3	.507	Aluminum
184.44	40	2.268	D_2O
185.93	3	.507	Aluminum
Fuel radius to cavity radius ratio, 0.530			
48.48	35	1.385	Fuel
91.46	5	8.596	Void
92.98	3	.507	Aluminum
184.45	40	2.268	D_2O
185.94	3	.507	Aluminum

TABLE II. - GEOMETRY AND MATERIALS FOR TWO-
DIMENSIONAL TRANSPORT CALCULATIONS

Distance to outer edge of region, cm	Number of mesh points	Width of mesh cell, cm	Material
Set 2, radial direction			
[a]81.38 [b]60.96 [c]48.43	8	[a]10.17 [b]7.62 [c]6.06	Fuel
91.44	4	[a]2.52 [b]7.63 [c]10.74	Void
92.66	2	.61	Aluminum
184.10	6	15.24	D_2O
185.32	2	.61	Aluminum
Set 2, axial direction			
1.22	2	0.61	Aluminum
92.66	5	18.29	D_2O
93.88	2	.61	Aluminum
215.80	11	11.08	Fuel
217.02	2	.61	Aluminum
308.46	5	18.29	D_2O
309.68	2	.61	Aluminum
Set 3, radial direction			
[a]81.38 [b]60.96 [c]48.46	8	[a]10.17 [b]7.62 [c]6.06	Fuel
91.44	4	[a]2.52 [b]7.63 [c]10.74	Void
185.32	10	9.39	D_2O + aluminum
Set 3, axial direction			
93.88	9	10.43	D_2O + aluminum
215.80	11	11.08	Fuel
309.68	9	10.43	D_2O + aluminum

[a]Fuel radius to cavity radius ratio, r_*, 0.890.
[b]$r_* = 0.667$.
[c]$r_* = 0.530$.

TABLE III. - GEOMETRY AND MATERIALS FOR ONE-

DIMENSIONAL TRANSPORT CALCULATIONS

Fuel radius to cavity radius ratio	Distance to outer edge of region, cm		Number of mesh points		Width of mesh cell, cm		Material
	I	II	I	II	I	II	
Set 4							
0.890	60.96	81.38	8	8	7.62	2.55	Fuel
.667	40.96	60.96	8	8	5.12	2.50	Fuel
.530	40.96	48.46	8	8	5.12	.94	Fuel
-----	91.44	-----	4	---	----	-----	Void
-----	103.44	185.32	12	8	1.00	10.24	D_2O + aluminum
Set 5							
0.900	70.00	82.30	8	4	8.75	3.08	Fuel
.890	73.00	81.38			9.13	2.09	
.875	70.00	80.01			8.75	2.50	
.850	70.00	77.72			8.75	1.93	
.825	70.00	75.44			8.75	1.36	
.800	60.00	73.15			7.50	3.29	
.775	60.00	70.87			7.50	2.72	
.750	60.00	68.58			7.50	2.15	
.700	60.00	64.00			7.50	1.00	
.667	56.00	60.69			7.00	1.17	
.650	54.00	59.44			6.75	1.36	
.600	50.00	54.86			6.25	1.22	
.550	46.00	50.29			5.75	1.07	
.530	44.00	48.46			5.50	1.12	
.500	40.00	45.72			5.00	1.43	
-----	91.44	------	4	---	----	-----	Void
-----	92.39	------	4	---	.24	-----	Aluminum
-----	102.39	181.29	10	8	1.00	9.87	D_2O
-----	182.24	------	4	---	.24	-----	Aluminum

Since the calculations did not consider the nozzle or air gap present in the experiment, the critical masses chosen for comparison required a correction for 1.25 percent excess reactivity Δk due to their removal (ref. 1). This was added to the already existing excess reactivity in each configuration. A 3-percent impurity content in the UO_2 foils was subtracted from the measured foil weight to get the uranium weight for the calculations.

Finally, a bias factor estimated by Henderson and Kunze (ref. 1) was applied in order to convert the critical foil mass to an equivalent critical mass for gaseous fuel.

TABLE IV. - EQUIVALENT CRITICAL MASS FOR GASEOUS FUEL

Fuel radius to cavity radius ratio	Actual fuel loading, kg U	Excess reactivity, Δk, percent	Fuel worth, $\dfrac{\Delta k/k}{\Delta m/m}$	Foil critical mass at k_{eff} = 1.00 kg U	Bias factor	Equivalent critical mass for gaseous fuel, kg U
0.890	10.7±0.1	1.46	0.331	10.3±0.1	1.35±0.05	7.6±0.3
.667	14.1±0.1	1.29	.255	13.4±0.1	1.21±0.05	11.1±0.5
.530	19.8±0.2	2.23	.182	17.4±0.2	1.13±0.05	15.4±0.8

The results of these steps are summarized in table IV.

The calculations are reported here in the order in which they were run. The first calculations used a one-dimensional diffusion theory code, which were followed by two-dimensional transport calculations in an effort to improve the results. When these did not achieve the accuracy desired due to computer storage limitations, the one-dimensional transport calculations were performed.

Following each set of calculations, the calculated k_{eff}, which were obtained by varying the fuel concentration, were plotted against their corresponding fuel masses, with the fuel radius to cavity radius ratio as a parameter. From these curves the critical masses at k_{eff} = 1.00 could be read for each radius ratio. These critical masses were then plotted against the radius ratio. This final graph permitted a comparison with another graph derived from experimental data.

Diffusion Calculations (Set 1)

The first calculations at Lewis were made with RP-4 a one-dimensional diffusion theory code. RP-4 uses 72 energy groups, including one thermal group. It obtains cross sections from its own library, has no up scattering and only one group scattering down.

For simplicity of calculations and to reduce the storage requirements of the computer code, a spherical geometry was used. Here the spherical dimensions were assumed to be equivalent to the radial dimensions of the cylindrical experiment configuration. The reactor was divided into the five regions which in turn were divided into 86 radial mesh intervals (see table I).

Two-dimensional diffusion calculations were not attempted. Hyland, Ragsdale, and Gunn (ref. 3) estimated that the computer time for an 80-centimeter radius cavity using only four energy groups would be 40 to 60 hours.

Two-Dimensional Transport Calculations

A two-dimensional discrete angular segmentation (Sn) transport code programmed in FORTRAN IV (ref. 4), called TDSN, performed all transport theory calculations. Both the one- and two-dimensional calculations reported here were limited to the S_4 angular flux approximation which has been shown to be sufficiently accurate (ref. 5).

The first set of two-dimensional transport calculations (set 2) employed the same cross sections as the diffusion calculations (set 1). These had no up scattering and one group down scattering, and they were collapsed to seven broad energy groups from the original 72 groups as follows:

Group number	Energy range
1	7. 79 MeV to 3. 68 MeV
2	3. 68 MeV to 1. 31 MeV
3	1. 31 MeV to 0. 15 MeV
4	. 15 MeV to 1. 13 eV
5	1. 13 eV to 0. 414 eV
6	. 414 eV to 0. 125 eV
7	. 125 eV to 0 eV

The two-dimensional capability of TDSN permitted a cylindrical geometry with 22 radial and 29 axial mesh points encompassing five regions.

The second group of two-dimensional calculations (set 3) differed from the first group (set 2) in several respects. A major difference was in the cross sections. GAM-II (ref. 6) provided the fast cross sections, while GATHER-II (ref. 7) supplied the thermal cross sections. The cross sections of the constituents of each material were flux weighted over the composition of their respective regions. These were combined with MACGG, a code written at Lewis for this purpose. The resulting cross section set had up and down scattering and a P_0 scatter transfer matrix. This is a set of scattering cross sections using a first-order approximation, that is, the P_0 terms of a Legendre polynomial. A P_1 scatter transfer matrix employs the second-order approximation, or the P_0 and P_1 terms of the Legendre polynominal (ref. 4). The cross sections were averaged over the following eight broad energy groups:

Group number	Energy range
1	14. 90 MeV to 2. 23 MeV
2	2. 23 MeV to 0. 82 MeV
3	. 82 MeV to 7. 10 keV
4	7. 10 keV to 0. 45 keV
5	. 45 keV to 0. 414 eV
6	. 414 eV to 0. 200 eV
7	. 200 eV to 0. 025 eV
8	. 025 eV to 0 eV

This set again used a cylindrical geometry, also with 22 radial and 29 axial mesh points. These, however, included only three regions, that is, the fuel, void, and moderator regions. The moderator region also contained the inner and outer tank wall besides the D_2O. The calculations in sets 2 and 3 considered values of the fuel radius to cavity radius ratio of 0. 890, 0. 667, and 0. 530.

One-Dimensional Transport Calculations

The one-dimensional transport calculations also consisted of two sets. The first one (set 4) used the same cross sections, energy groups, and regions as set 3 of the two-dimensional calculations. The only change was to a spherical geometry with 40 radial meshpoints, and the fuel and D_2O regions were subdivided into two regions each. The inner and outer subregions are labeled I and II, respectively, in table III. These subregions permit closer mesh spacing at the fuel-void and D_2O-aluminum-void boundaries where the flux gradient is large. This results in an improved neutron flux calculation. The radius ratios for set 4 were 0. 890, 0. 667, and 0. 530.

The cross sections in set 5 were also obtained from GAM-II and GATHER-II. These, however, were P_1 cross sections. Again, a spherical geometry was used, this time with 42 radial meshpoints. The fuel and D_2O regions were subdivided to give the following 7 regions: (1), (2) fuel, (3) void, (4) inner aluminum tank, (5), (6) D_2O, and (7) outer aluminum tank. The radius ratios ranged from 0. 500 to 0. 900. The number of broad energy groups was increased to 20, with ten fast and ten thermal groups, having up scattering in the thermal groups and down scattering to all groups. The energy groups had the following ranges.

Group number	Energy range	Group number	Energy range
1	14.720 MeV to 3.012 MeV	11	2.382 eV to 1.600 eV
2	3.012 MeV to 2.019 MeV	12	1.600 eV to 1.200 eV
3	2.019 MeV to 1.225 MeV	13	1.200 eV to 0.850 eV
4	1.225 MeV to 0.608 MeV	14	0.850 eV to 0.330 eV
5	.608 MeV to 2.035 keV	15	0.330 eV to 0.220 eV
6	2.035 keV to 0.275 keV	16	0.220 eV to 0.100 eV
7	.275 keV to 61.440 eV	17	0.100 eV to 0.025 eV
8	61.440 eV to 10.680 eV	18	0.025 eV to 0.010 eV
9	10.680 eV to 3.928 eV	19	0.010 eV to 0.005 eV
10	3.928 eV to 2.382 eV	20	0.005 eV to 0 eV

RESULTS

Diffusion Calculations

The diffusion calculations produced critical masses lower than the experiment (table V, and figs. 2 and 3). This has been the experience at Lewis in other cavity reactor calculations using diffusion theory codes. When comparing the deviation of the calculated critical masses from the experimental critical masses, one can see that the deviation varies inversely with fuel radius to cavity radius ratio, or directly with the cavity void fraction. This result can be traced to two causes. First, the diffusion

TABLE V. - RESULTS OF DIFFUSION CALCULATIONS

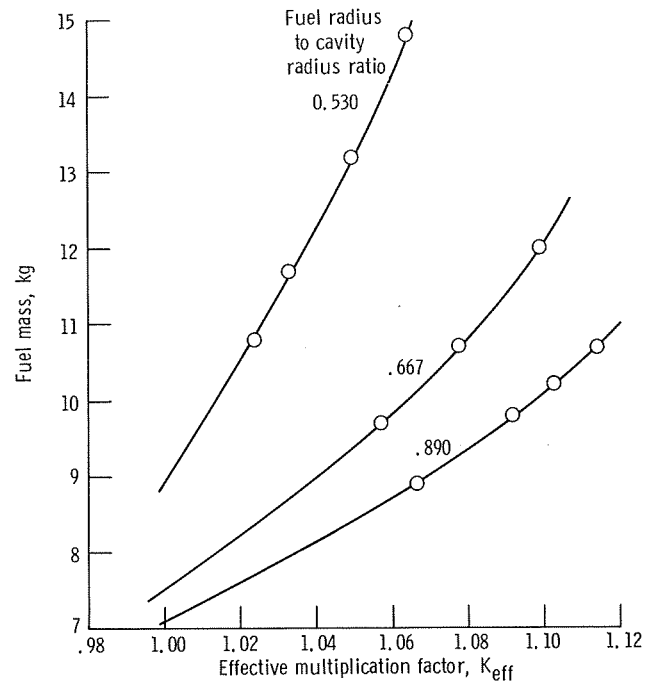| Fuel radius to cavity radius ratio	Fuel mass, kg	Calculated, k_{eff}	Extrapolated critical mass (k_{eff} = 1.00), kg
0.890	8.9	1.0666	
	9.8	1.0919	7.1
	10.2	1.1027	
	10.7	1.1142	
0.667	9.7	1.0570	
	10.7	1.0774	7.5
	12.0	1.0989	
0.530	10.8	1.0239	
	11.7	1.0331	8.9
	13.2	1.0496	
	14.8	1.0640	

Figure 2. - Effective multiplication factor as function of fuel mass.
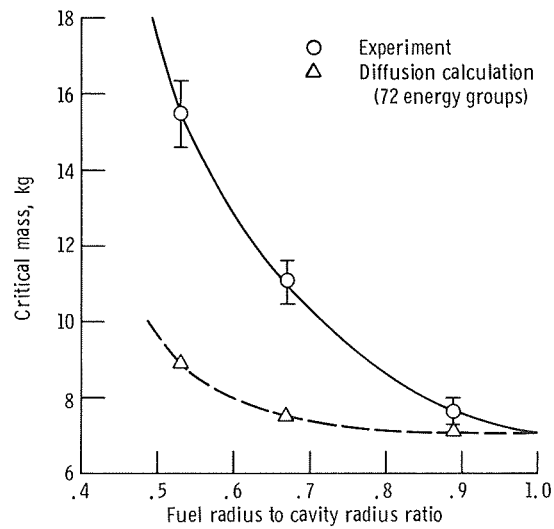One-dimensional diffusion calculations; 72 energy groups.

Figure 3. - Critical mass as function of fuel radius to
cavity radius ratio. Diffusion calculation; experi-
ment comparison.

theory codes cannot handle the large voids which exist at small fuel-radius to cavity-radius ratios. The second, a geometry problem, compounds the error.

Here the difficulty lies in trying to simulate a cylinder with a sphere. The problem arises in the fuel region, where the length to diameter ratio varies. Typical values for the length to diameter ratio are 3/4, 1/1, and 5/4 for radius ratios of 0.890, 0.667, and 0.530, respectively. A sphere can be expected to simulate a cylinder well if the length to diameter ratio is near 0.9; that is, the radius ratio is near 0.740. This geometry problem at small radius ratios also arose for the one-dimensional transport calculations.

Each diffusion calculation required 12 to 15 minutes of computer time.

Two-Dimensional Transport Calculations

Both sets of the two-dimensional transport calculations resulted in critical masses 50 to 100 percent higher than the experimental critical masses (see table VI and figs. 4 to 6). The deviation increased rapidly for radius ratios smaller than 0.600.

TABLE VI. - RESULTS OF TWO-DIMENSIONAL

TRANSPORT CALCULATIONS

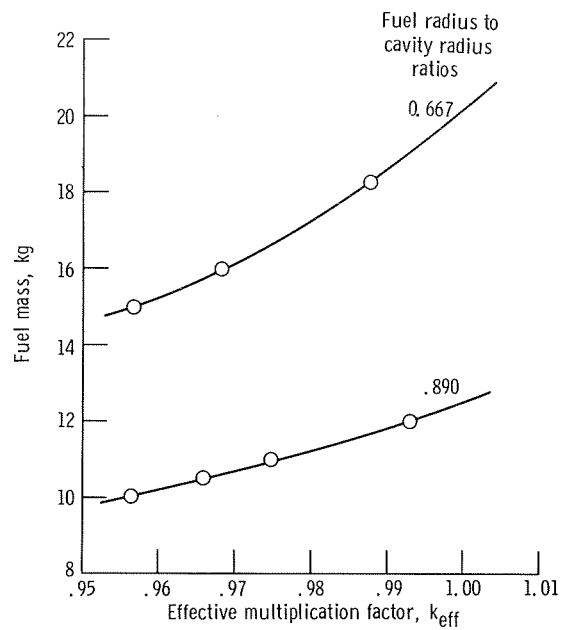| Fuel radius to cavity radius ratio	Fuel mass, kg	Effective multiplication factor, k_{eff}		Critical mass, kg	
		Set 2	Set 3	Set 2	Set 3
0.890	10.0	0.9476	0.9566	}12.6	12.5
	10.5	------	.9660		
	11.0	.9730	.9747		
	11.5	.9830	------		
	11.8	.9888	------		
	12.0	.9897	.9930		
0.667	14.5	0.9762	------	}16.9	20.2
	15.0	------	0.9569		
	16.0	.9927	.9682		
	17.5	1.0045	------		
	18.0	1.0072	------		
	18.3	------	.9876		
	19.0	1.0155	------		
0.530	20.6	0.9657	------	}30.2	32^{+}
	22.0	.9725	0.9643		
	25.0	.9845	------		
	28.0	.9935	------		

Figure 5. - Effective multiplication as function of fuel
mass. Two-dimensional transport calculations;
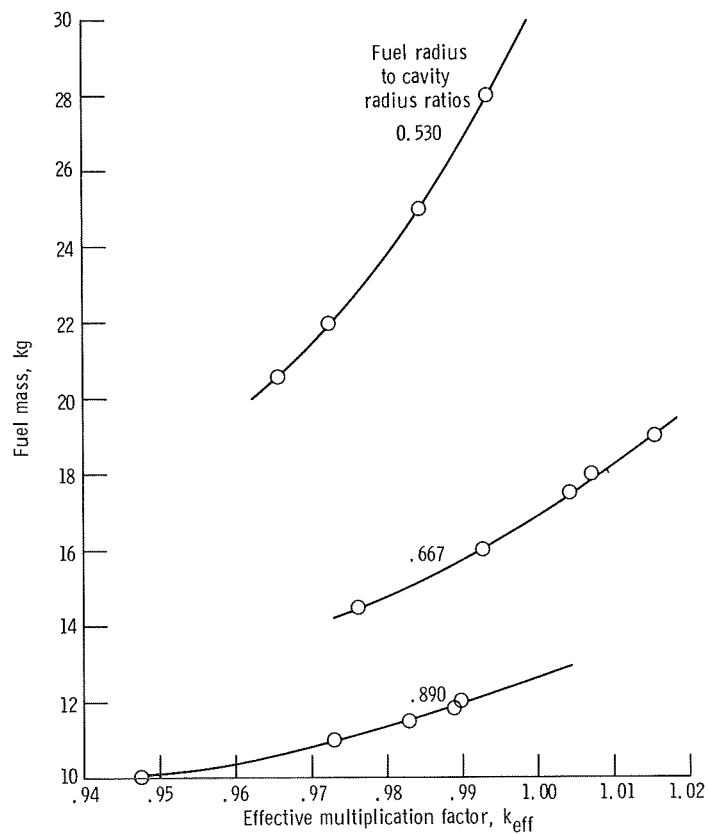eight energy groups.

Figure 4. - Effective multiplication factor as function of fuel mass. Two-
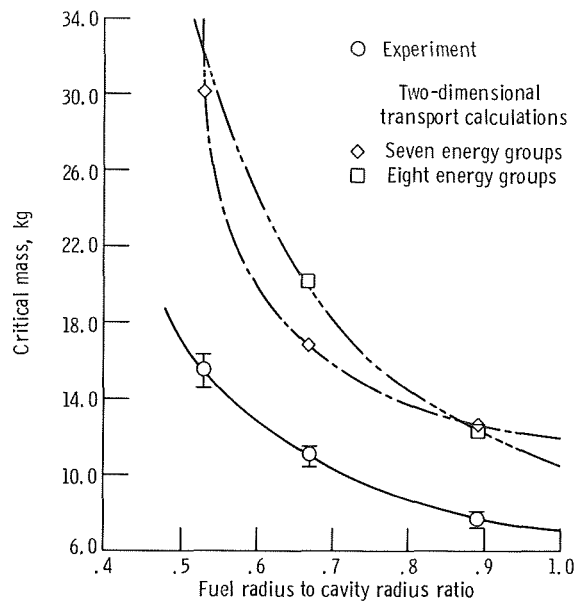dimensional transport calculations; seven energy groups.

Figure 6. - Critical mass as function of fuel radius to cavity radius ratio. Two dimensional transport calculations; experiment comparison.

The addition of more groups, especially thermal groups, and up and down scattering improves the accuracy of the calculations. However, this is counteracted by the detrimental effect of reducing the number of regions and mesh points. Based on a comparison between sets 3 and 4, the overall result is to increase the error of the calculation, particularly for fuel-radius to cavity-radius ratios less than 0.850.

Henderson and Kunze (ref. 1) indicate that the mesh spacing in the reflector is the most critical. Here the large out-scattering cross sections result in very short mean free paths. These are about 2 centimeters for thermal neutrons. A rule of thumb for establishing mesh interval size is that it should be equal to or less than the mean free path in the material. All regions of every set meet this criterion except the D_2O region in sets 2 and 3. Here the mesh spacing is from 5 to 8 times the mean free path. This is the most likely source of error for the two-dimensional calculations.

Increasing the number of mesh points should produce greater accuracy, but, for a reactor as large as the one considered here, core storage requirements limit the number of mesh points permissible for two-dimensional calculations. The storage required is a function of the number of energy groups, materials, up and down scattering transfers, and geometry. At the storage limit, an increase in any of these quantities

requires a corresponding decrease in the number of one or more of the others. For any particular configuration, it should be possible to find an optimum combination of input parameters by trial and error, but this is a costly process since the computer time ranges from 150 to 900 minutes per calculation. It would probably be less costly and time consuming to determine the effect of changing each variable by doing one-dimensional calculations with TDSN before switching to two-dimensional calculations. Such a procedure, however, was not considered within the scope of this study.

One-Dimensional Transport Calculations

The results of the one-dimensional calculations show that the critical masses again were overestimated (tables VII and VIII, figs. 7 to 11). The results (of the calculations in set 4) were more accurate than those of set 3, the two-dimensional calculations, which were identical except for cylindrical geometry and a smaller number of mesh points. This points out the importance of good spatial detail in the model. Again, the mean free paths were smaller than the mesh intervals for every region except the outer subregion of the D_2O. The same geometry problem described in the results of the diffusion calculations was also noted in these calculations. The greater accuracy in the calculations of set 5 is due to the greater number of energy groups, the thermal groups in particular, the use of the P_1 scatter-transfer matrix, and better definition of mesh points at the fuel-void and D_2O-aluminum-void boundaries, where large flux gradients exist.

The computer program running times for set 4 calculations ranged from 15 to 30 minutes, while in set 5, the computer required from 28 to 32 minutes for a calculation.

TABLE VII. - RESULTS OF ONE-DIMENSIONAL

TRANSPORT CALCULATIONS

[Data for set 4.]

Fuel radius to cavity radius ratio	Fuel mass, kg	Effectively multiplication factor, k_{eff}	Critical mass, kg
0.890	9.80 10.70	0.9794 .9979	10.8
0.667	8.95 10.60 12.10	0.8918 .9250 .9492	16.1
0.530	11.80	0.8610	~27.0

16

TABLE VIII. - RESULTS OF ONE-DIMENSIONAL

TRANSPORT CALCULATIONS - SET 5

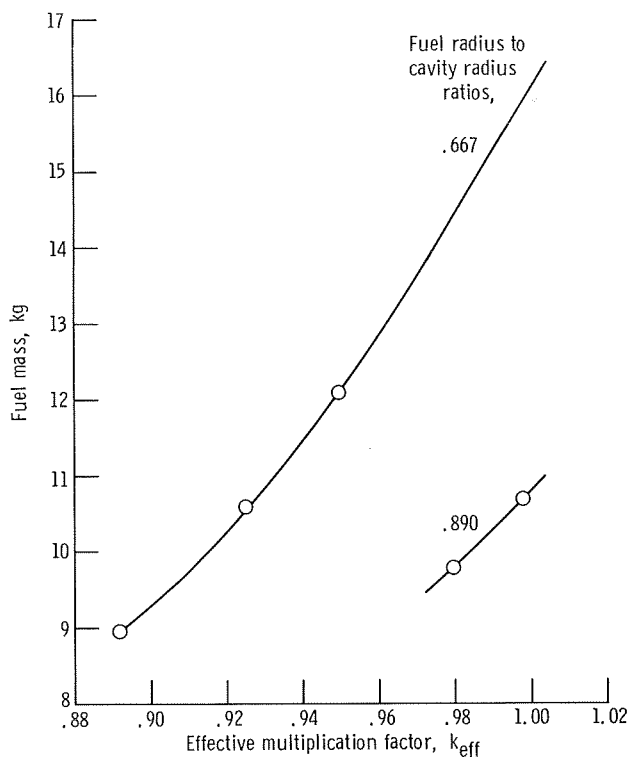| Fuel radius to cavity radius ratio	Fuel mass, kg	Effective multiplication factor, k_{eff}	Extrapolated critical mass, kg
0.900	9.25	1.0285	~8.4
.890	11.00	1.0666	~8.4
.875	11.00	1.0633	~8.5
.850	9.25	1.0156	
.850	10.00	1.0366	8.7
.850	11.00	1.0567	
.825	10.00	1.0292	9.1
.800	9.25	1.0000	
.800	10.00	1.0225	9.3
.800	11.00	1.0418	
.775	10.00	1.0123	9.5
.750	11.00	1.0250	9.9
.750	12.50	1.0381	
.700	11.00	1.0060	
.700	12.50	1.0162	10.9
.700	13.50	1.0312	
.700	14.50	1.0435	
.667	12.50	.9950	12.8
.667	13.50	1.0093	
.650	14.50	1.0153	
.650	17.50	1.0480	13.2
.650	20.40	1.0679	
.600	14.50	.9809	
.600	17.50	1.0120	
.600	20.40	1.0302	16.2
.600	30.00	1.0700	
.550	20.40	.9878	23.8
.550	30.00	1.0225	
.530	30.00	.9983	30.2
.500	20.40	.9302	----

Figure 7. – Effective multiplication factor as function of fuel mass.
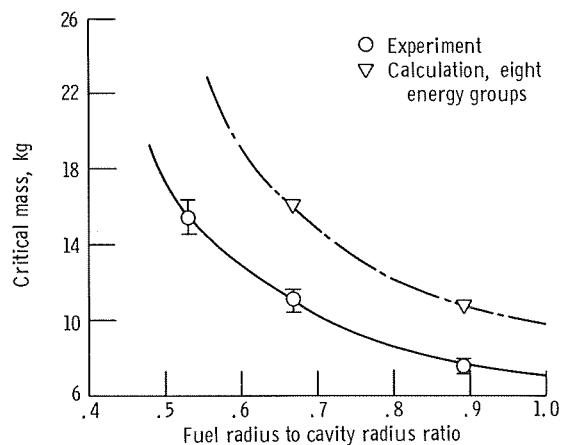One-dimensional transport calculations; eight energy groups.

Figure 8. – Critical mass as function of fuel radius to
cavity radius ratio. One-dimensional transport
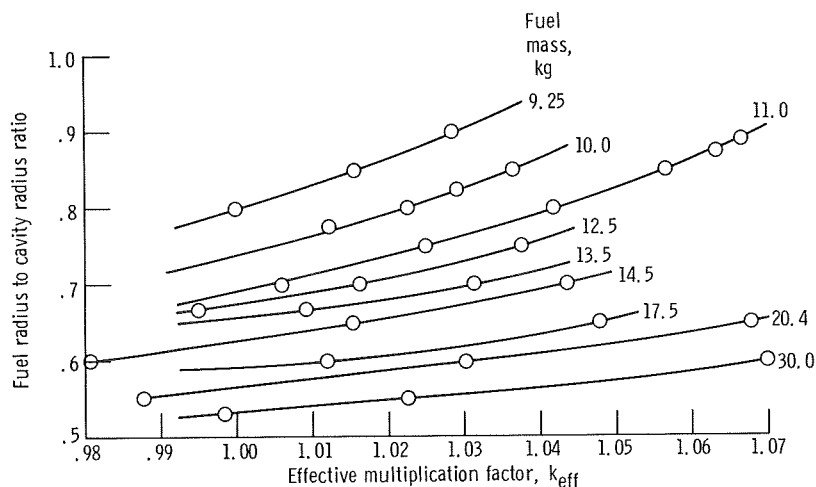calculation; experiment comparison.

Figure 9. – Fuel radius to cavity radius ratio as function of effective multiplica-
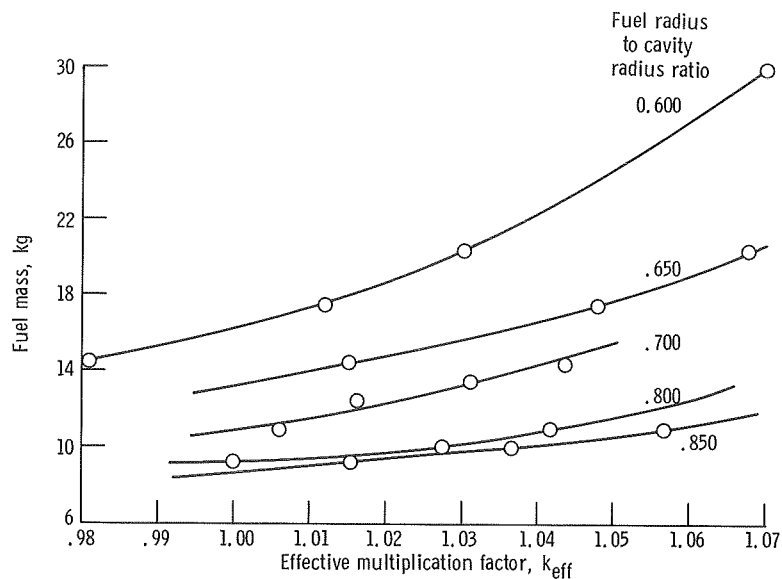tion factor. One-dimensional transport calculations; 20 energy groups.

Figure 10. - Fuel mass as function of effective multiplication factor. One-dimensional transport calculations; 20 energy groups.
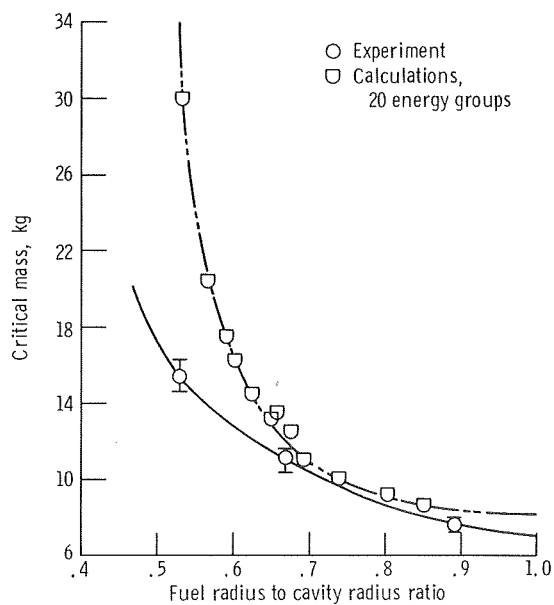

Figure 11. - Critical mass as function of fuel radius to cavity radius ratio. One-dimensional transport calculation; experiment comparison.

SUMMARY OF RESULTS

Calculated critical masses for a gas-core cavity reactor were compared with critical masses determined in an experiment. Three methods of calculations were used: (1) one-dimensional diffusion theory, (2) one-dimensional transport theory, and (3) two-dimensional transport theory. The mesh spacing, material distribution, and number of energy groups were varied among these to produce five distinct sets of calculations. These had the following results:

1. One-dimensional diffusion calculations underestimate critical masses. These calculations are good for fuel-radius-to-cavity-radius ratios near 1.0, but become increasingly inaccurate as the fuel becomes more compressed and the void fraction of the cavity increases. This makes them unsatisfactory for gas core cavity reactor calculations, as these reactors are expected to have large void fractions. These calculation required the least computer time, however.

2. Transport calculations overestimated critical masses. They provided better results than diffusion calculations at smaller radius ratios, although for radius ratios smaller than 0.600, the error increased rapidly for all types of calculations.

3. For computers with core storage and execution time limits, one-dimensional transport calculations produced better results than two-dimensional calculations. This is due to the greater refinement, that is, number of energy groups, mesh points, etc., possible with a one-dimensional geometry. The one-dimensional calculations also provided a decrease in computer time by a factor of 10 over the two-dimensional calculations.

4. The accuracy of transport calculations was improved by increasing the number of energy groups, thermal groups in particular, and by reducing the mesh spacing. Further gains in accuracy were achieved by a better definition of materials distribution, that is, adding regions, and by using a P_1 scatter-transfer matrix instead of P_0.

Lewis Research Center,
    National Aeronautics and Space Administration,
        Cleveland, Ohio, May 8, 1970
           122-29.

REFERENCES

1. Henderson, W. B.; and Kunze, J. F.: Analysis of Cavity Reactor Experiments. Rep. GEMP-689, General Electric Co. (NASA CR-72484), Jan. 1969.

2. Pincock, G. D.; and Kunze, J. F.: Cavity Reactor Critical Experiment. Vol. 1. General Electric Co. (NASA CR-72234), Sept. 6, 1967.

3. Hyland, Robert E.; Ragsdale, Robert G.; and Gunn, Eugene J.: Two-Dimensional Criticality Calculations of Gaseous-Core Cylindrical-Cavity Reactors. NASA TN D-1575, 1963.

4. Barber, Clayton E.: A FORTRAN IV Two-Dimensional Discrete Angular Segmentation Transport Program. NASA TN D-3573, 1966.

5. Miraldi, Floro; Nelson, George W.; Holmberg, Gary; and Skoff, Gerald: Neutron Flux Distributions: (Experiment vs. Theory) for a Water Reflected-Spherical Cavity System. Case Inst. Tech. (NASA CR-72231), Dec. 31, 1966.

6. Joanou, G. D.; and Dudek, J. S.: GAM-II. A B_3 Code for the Calculation of Fast Neutron Spectra and Associated Multigroup Constants. Rep. GA-4265, General Atomics Div., General Dynamics Corp., Sept. 16, 1963.

7. Joanou, G. D.; Smith, C. V.; and Vieweg, H. A.: GATHER-II. An IBM-7090 FORTRAN II Program for the Computation of Thermal Neutron Spectra and Associated Multigroup Cross Sections. Rep. GA-4132, General Atomics Div., General Dynamics Corp., July 8, 1963.

"The aeronautical and space activities of the United States shall be conducted so as to contribute . . . to the expansion of human knowledge of phenomena in the atmosphere and space. The Administration shall provide for the widest practicable and appropriate dissemination of information concerning its activities and the results thereof."

— NATIONAL AERONAUTICS AND SPACE ACT OF 1958

NASA SCIENTIFIC AND TECHNICAL PUBLICATIONS

TECHNICAL REPORTS: Scientific and technical information considered important, complete, and a lasting contribution to existing knowledge.

TECHNICAL NOTES: Information less broad in scope but nevertheless of importance as a contribution to existing knowledge.

TECHNICAL MEMORANDUMS: Information receiving limited distribution because of preliminary data, security classification, or other reasons.

CONTRACTOR REPORTS: Scientific and technical information generated under a NASA contract or grant and considered an important contribution to existing knowledge.

TECHNICAL TRANSLATIONS: Information published in a foreign language considered to merit NASA distribution in English.

SPECIAL PUBLICATIONS: Information derived from or of value to NASA activities. Publications include conference proceedings, monographs, data compilations, handbooks, sourcebooks, and special bibliographies.

TECHNOLOGY UTILIZATION PUBLICATIONS: Information on technology used by NASA that may be of particular interest in commercial and other non-aerospace applications. Publications include Tech Briefs, Technology Utilization Reports and Notes, and Technology Surveys.

Details on the availability of these publications may be obtained from:

SCIENTIFIC AND TECHNICAL INFORMATION DIVISION

NATIONAL AERONAUTICS AND SPACE ADMINISTRATION
Washington, D.C. 20546